Lateral piezoelectric fields in strained semiconductor heterostructures

Matthias Ilg and Klaus H. Ploog
Paul-Drude-Institut für Festkörperelektronik, Hausvogteiplatz 5-7, D-10117 Berlin, Germany

Achim Trampert
Max-Planck-Institut für Festkörperforschung, Heisenbergstrasse 1, D-70569 Stuttgart, Germany
(Received 8 July 1994)

Lateral piezoelectric fields exist in almost all strained III-V semiconductor quantum wells. We first discuss the origin of the lateral fields and point out their most important features. Then the controlled creation of lateral piezofields is demonstrated using a series of (110) InAs/GaAs quantum-wire structures. After verification of the structural perfection by high-resolution x-ray diffraction and transmission electron microscopy an optical study unambiguously demonstrates the existence of lateral fields. By increasing the excitation density in photoluminescence experiments we observe pronounced blueshifts of the luminescence lines simultaneously with a clear reduction of the linewidths. Additional evidence comes from time-resolved measurements where a strong dependence of the radiative lifetime on energy is observed. These results are supported by a study of strained structures with other orientations. In (211), (311), and (210) samples we find evidence of lateral piezofields created by interface fluctuations. Our results show that the impact of lateral piezoelectric fields has to be taken into account in any fundamental analysis of strained III-V semiconductor heterostructures. Furthermore, lateral piezoelectric fields represent a different concept to achieve artificial materials with strong optical nonlinearities.

I. INTRODUCTION

A strong piezoelectric polarization exists in strained III-V heterostructures with non-[100] orientation.[1] This polarization normally splits up in a component in growth direction and a component parallel to the interfaces.[2] In ideal quantum wells, without any lateral features, only the vertical component creates polarization charges and hence electric fields. Research activities up to now have focused exclusively on these vertical electric fields.[3–10]

The inactivity of the polarization component parallel to the interfaces, however, can be lifted by a lateral structuring of the quantum well. The parallel polarization component then also generates piezoelectric charges and it introduces lateral piezoelectric fields. The magnitude of these lateral fields and their impact on the potential profile of the heterostructure can be significantly larger than that of vertical fields. Furthermore, lateral fields are normally created by a much smaller total amount of piezoelectric charge and, therefore, can be screened more easily. As a result, lateral piezoelectric fields have an extremely strong impact on the optical properties of strained III-V heterostructures and open up an avenue to large nonlinear-optical effects. Therefore, lateral fields are of highest interest for device applications. And they have a crucial impact on fundamental studies, since real heterostructures always exhibit interface fluctuations and hence lateral fields are almost always present in strained III-V heterostructures. It is therefore mandatory for any study of the optical and electronic properties of such structures to take into account the influence of lateral piezoelectric fields.

This paper is organized as follows. We start with a theoretical section in which we describe the concept of lateral piezoelectric fields and summarize the differences between lateral and vertical fields. Since lateral field effects are strongest in [110] oriented samples,[2] we first focus on the experimental investigation of InAs quantum-wire structures in a (110) GaAs matrix. A detailed structural analysis of our set of (110) samples and (100) reference samples by high-resolution double-crystal x-ray diffraction (HRDXD) and transmission electron microscopy (TEM) reveals high structural perfection. Using different spectroscopic methods, we unambiguously demonstrate the presence of lateral piezofields and their strong impact on the optical properties of these samples. These results are then supported by a spectroscopic investigation of strained structures with various other non-[100] orientations.

II. THEORETICAL CONSIDERATIONS

In piezoelectric compounds with a zinc-blende structure a relation exists between the off-diagonal elements of strain tensor ϵ_{jk} and the vector P_i of the piezoelectric polarization via the piezoelectric constant e_{14}:[11]

$$P_i = 2e_{14}\epsilon_{jk} \ . \tag{1}$$

As illustrated in Fig. 1, the strained layer of material B on a high-symmetry (100) substrate of material A exhibits neither a piezoelectric polarization nor any electric fields. In the (111) structure, the polarization is perpendicular to the interface. It thus creates polarization charges and an electric field. We subsequently refer to this situation as "vertical field case." In an *ideal* (110) sample the polarization is parallel to the interfaces and hence no electric field exists. For a general (hkl) orientation the polarization has components parallel and perpendicular to the in-

 ©1994 The American Physical Society

terfaces. Therefore, in general, we always have piezoelectric charges and fields *as well as* a lateral component of the polarization.

Figure 2 illustrates the quantitative aspects of Eq. (1) using the example of a strained InAs layer in an unstrained GaAs matrix. In Fig. 2(a), the magnitude of the polarization vector is shown for all substrate orientations between [001] and [110].[12] It is important for the work presented here that the magnitude of the polarization vector remains virtually constant for the orientations between [111] and [110]. In the InAs/GaAs system under discussion the polarization charge density created at the interfaces in a (111) structure is about 3×10^{11} cm^{-2}. Going from the [111] to the [110] directions, this charge density drops to zero because the polarization vector gradually rotates into the plane of the interfaces. Therefore, we get a clear maximum of the electric-field strength for the [111] direction [see Fig. 2(b)] with a value of 4×10^5 V/cm. This work, however, is concerned with the lateral component of the polarization vector, which is plotted in Fig. 2(c). It exhibits maxima for the (110) case as well as for an orientation between [211] and [311].

We now turn to the central observation of this work. In the ideal (110) quantum well depicted in Fig. 3(a), the lateral component of the polarization does not pierce any interfaces. It, consequently, cannot create any piezoelectric charges nor piezoelectric fields. However, the situation changes dramatically when we look at the boundary conditions introduced to the electrostatic problem by a real quantum well as shown in Fig. 3(b). Due to interface roughness, the lateral polarization component has the possibility to penetrate the interfaces. Piezoelectric charges are created and piezoelectric fields introduced. Figure 3(c) finally illustrates the possibility of engineered

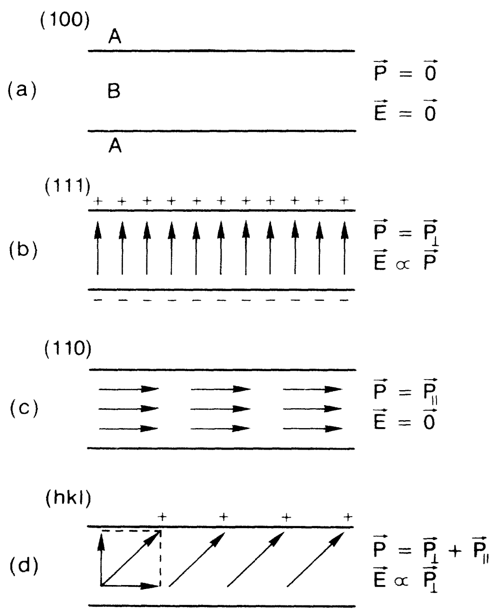

FIG. 1. Polarization, electrical charges, and fields in a strained *B* layer on an *A* substrate for (a) [100], (b) [111], and (c) [110] orientation. (d) Shows the general case of a (*hkl*) heterostructure.

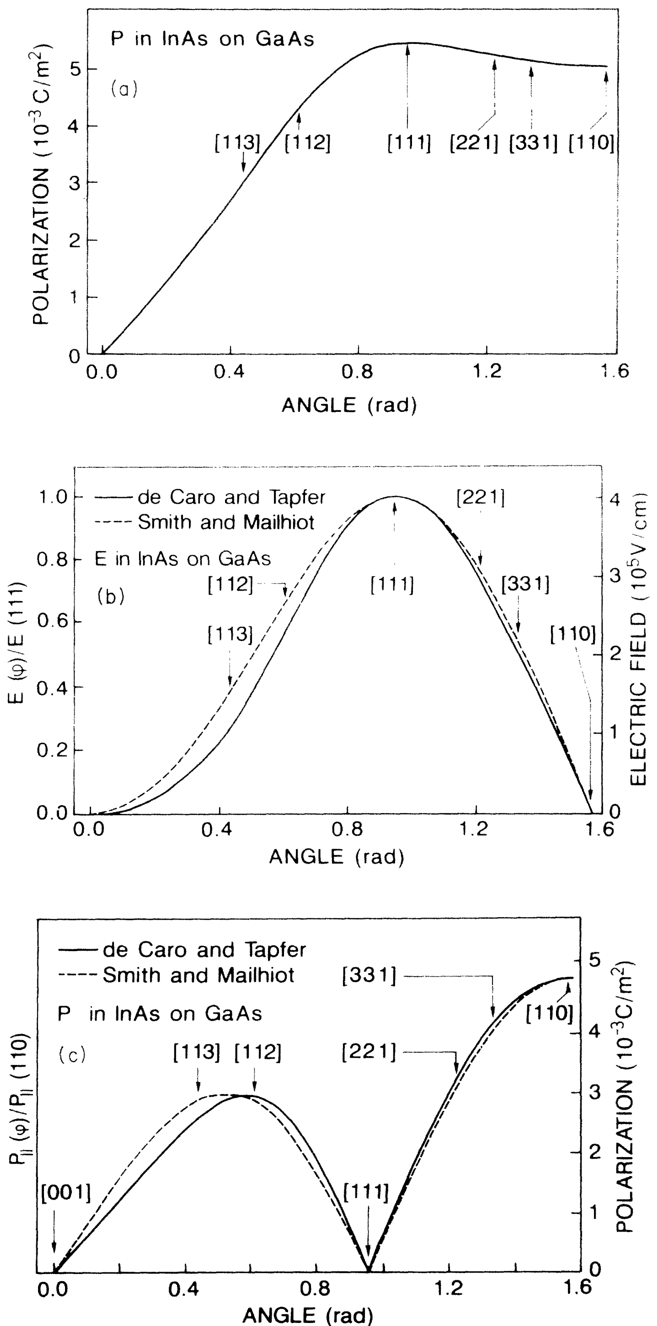

FIG. 2. Magnitude of the piezoelectric polarization vector (a), the piezoelectric field (b), and the lateral polarization component (c) in a pseudomorphically strained InAs layer on GaAs substrates of various orientations. The values for the strain tensor elements have been calculated according to de Caro and Tapfer (Ref. 13) and Smith and Mailhiot (Ref. 2) with and without shear strain effects, respectively.

lateral piezoelectric fields by the growth of strained structures on vicinal surfaces.

All experimentally accessible structures are real quantum wells. They, therefore, always exhibit lateral features in the form of interface roughness. Also a lateral polarization component is always present in any strained III-V or II-VI heterostructure unless the growth direction coincides with the exceptional [100] and [111] directions. *Therefore, lateral piezoelectric fields are a universal feature of strained III-V semiconductor heterostructures. Their presence has to be taken into account in any fundamental analysis of the electronic and optical properties of such structures.*

What are the specific properties of lateral piezoelectric fields and what are the differences between lateral and vertical fields? These questions can be answered best by discussing a representative example which exhibits all the characteristic features of lateral piezoelectric fields. The key points of the comparison between lateral and vertical electric fields carried out below are summarized in Table I. As a model system, we select an array of strained $In_{0.5}Ga_{0.5}As$ quantum wires on (110) GaAs with the wires running in the $[1\bar{1}0]$ direction. The piezoelectric polarization in the strained (In,Ga)As wires points in the [001] direction and therefore creates charges on the wire edges. We select the lateral quantum-wire width w and the period Λ of the array to be 200 Å, the thickness of the wires in growth direction d is 4 Å. The wires are assumed to form a staircaselike array as can be expected on a vicinal surface. The electrostatic potential of this charge distribution can be approximated by the expression for an infinite array of line charges with alternating sign. Therefore, the following term[14] has to be superimposed with the quantum-wire potential:

$$\Phi_{\text{piezo}} = \frac{\lambda}{2\pi\epsilon_0\epsilon_r} \sum_{n=-\infty}^{n=+\infty} \ln(\mathbf{r}_{n+}) - \ln(\mathbf{r}_{n-}) \ . \tag{2}$$

$\mathbf{r}_{n+}$ and $\mathbf{r}_{n-}$ represent the positions of positive and negative charges at the nth wire. The line-charge density λ of the piezocharges is the product of polarization charge density and the wire thickness d. Figure 4 shows the po-

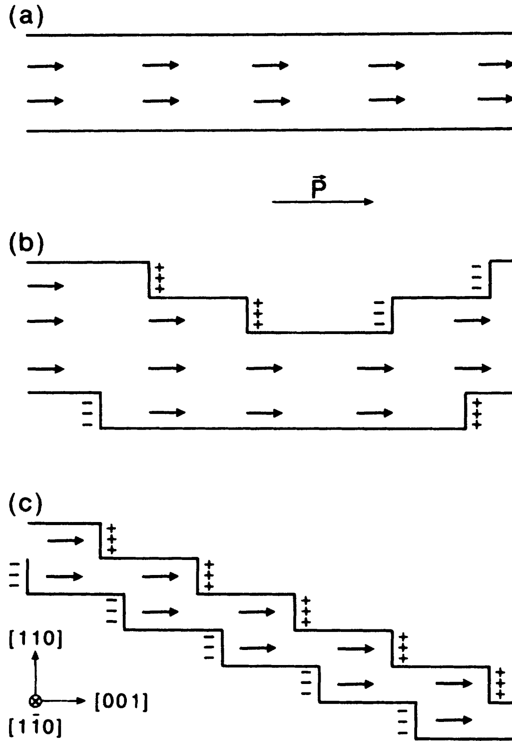

FIG. 3. Impact of a lateral polarization on different quantum-well geometries illustrated for the case of a [110] oriented, strained heterostructure with the polarization vector **P** pointing in the [001] direction. In an *ideal* heterostructure (a), we have no interface fluctuations and, therefore, **P** cannot create any interface charges. In a *real* heterostructure (b), however, interface fluctuations always exist and, therefore, surface charges are introduced. Since for strained heterostructures with general orientation **P** is expected to have a lateral component (Ref. 2); lateral piezofields are a universal phenomenon in strained semiconductor heterostructures made from III-V and II-VI semiconductors. (c) finally demonstrates the controlled introduction of interface charges by the use of vicinal surfaces.

without piezoelectric field:

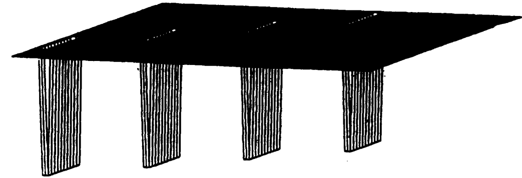

with piezoelectric field:

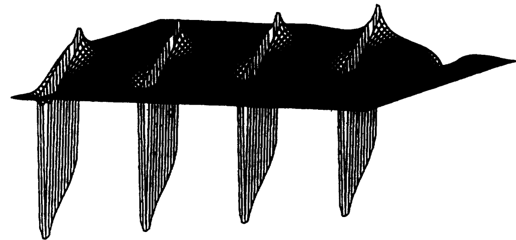

FIG. 4. Potential surface of a $[01\bar{1}]$ cross section through a (110) $In_{0.5}Ga_{0.5}As$ quantum-wire structure with and without lateral piezoelectric fields. The wire width is 200 Å and the thickness 4 Å. The potential term Φ_{piezo} was multiplied by a factor of 5 for illustrative purposes.

TABLE I. Comparison of vertical and lateral piezoelectric fields. The numbers given are for the (111) InAs/GaAs (vertical fields) and (110) InAs/GaAs systems (lateral fields).

Feature	Vertical fields	Lateral fields
Type of charge distribution	2D: charge sheets	1D: line charges
Areal charge density	$\sigma = P$, 3×10^{12} cm^{-2}	$0<\sigma<P$, typically 10^{10}–10^{11} cm^{-2}
Spatial distribution of fields	Spatially homogeneous within one constituent: plate-capacitor case. Always zero field in unstrained material	Irregular, with logarithmic singularities. Nonzero field strength in unstrained material.
Field strength	$E=\frac{P}{\epsilon_0\epsilon_r}$, 4×10^5 V/cm	$0<E<\infty$
Potential drop between positive and negative charges	Limited by critical thickness of strained layer	Unlimited

tential profile of the quantum-wire array with and without piezoelectric field. With the field we get potential singularities around the wire edges. Lateral fields, therefore, can have locally much larger field strengths than vertical fields. The presence of piezocharges leads to a bending of the bands inside the $In_{0.5}Ga_{0.5}As$ quantum wires. We even observe changes of the potential outside the wires in the unstrained GaAs barrier. In contrast, vertical fields are nonzero only in strained parts of the heterostructure.

The impact of the lateral fields on potential profile and optical matrix elements can be made arbitrarily large by an appropriate choice of quantum-wire width w and period Λ. For vertical fields, however, the critical thickness of the strained layer determines the largest possible separation of negative and positive charges and hence the impact of the electric field.

The charges producing lateral piezoelectric fields are of the line-charge type,[15] whereas vertical fields are generated by charge sheets. In the case of lateral fields, we therefore have a one-dimensional (1D) and in the case of vertical fields a two-dimensional (2D) charge distribution. Therefore, the average areal charge density for lateral fields (for quantum wires $\sigma = dP/\Lambda$) is, in general, significantly smaller than for vertical fields. In our theoretical example, we have an areal charge density of only 7×10^{10} cm^{-2} whereas for a similar (111) structure, this value is 3.5×10^{12} cm^{-2}, i.e., almost two orders of magnitude larger. We point out that the total number of states of InAs or $In_xGa_{1-x}As$ wells with comparable confinement energy is only of the order 10^{12} cm^{-2}. Consequently, a full screening of the vertical field requires a complete filling of the quantum well and hence extremely high optical excitation densities. In contrast to that, the screening of the lateral fields and with that the full exploitation of the nonlinear possibilities can be achieved at much smaller optical excitation densities. With a different choice of the quantum-wire width and the period of the wire array, we can easily obtain areal charge densities even smaller than in our theoretical example.

To conclude the theoretical section, we emphasize that lateral fields promise larger electric-field effects than vertical fields. Simultaneously they can be screened at significantly smaller optical excitation densities. These properties make lateral piezoelectric fields extremely interesting and allow the creation of artificial materials with highly nonlinear optical response.

III. EXPERIMENTAL RESULTS

A. Setup

We use solid-source molecular-beam epitaxy (MBE) to synthesize our structures on (110), (110), (311), (211), and (210) GaAs substrates. The (110) substrates have a 7° misorientation towards the [111] direction. The non-(100) substrates are soldered side by side with the (100) reference structure on a Mo holder using In. The growth process is monitored *in situ* by means of reflection high-energy electron diffraction (RHEED). Before starting the growth the native oxide of the GaAs surface is desorbed at 580 °C under impinging As_4 flux. The GaAs and InAs growth rates are 2 Å/s and 0.2 Å/s, respectively. High-resolution double-crystal x-ray diffraction is performed with a double-crystal x-ray diffractometer in Bragg geometry. A rotating-anode 12-kW generator with a copper target is employed as x-ray source, and an asymmetrically cut (100) Ge crystal serves as monochromator and collimator. The diffraction patterns are recorded in the vicinity of the symmetrical GaAs (400), (311), (422), and (220) reflections. The TEM images are obtained in a JEOL 4000FX electron microscope operating at 400 kV. For the PL experiments, the samples are mounted in an optical flow-through cryostat at 6 K and excited by the red line (647.6 nm) of a Kr^+ laser. The emitted light is focused on the entrance slit of a 1-m single-grating monochromator and detected by a photomultiplier in the photon-counting mode. Time-resolved PL experiments are carried out under pulsed excitation with an Ar^+-laser pumped Ti:sapphire laser. The emission is dispersed by a 32-cm spectrometer, followed by a Hamamatsu 2D streak camera with a time resolution of 10 ps.

B. InAs quantum-wire structures on GaAs (110)

From the theoretical section, we know that lateral piezoelectric fields are strongest for (110) heterostruc-

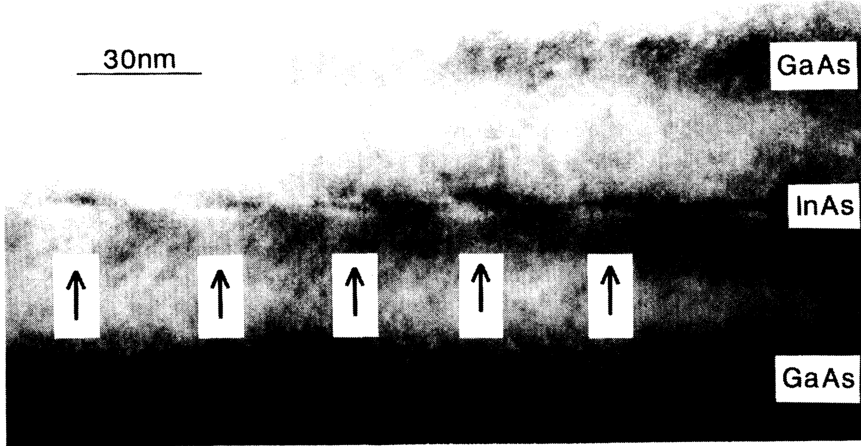

FIG. 5. TEM micrograph of the 3-Å (110) sample realizing the quantum-wire structure. The lateral periodicity of 300 Å of the InAs quantum wires can be seen clearly.

tures. It is a fortunate coincidence that the [110] and neighboring orientations exhibit a pronounced tendency for step bunching during epitaxial growth and thus allow *in situ* lateral patterning.[16–19] As demonstrated by Fig. 5, the choice of (110) substrates with a 7° miscut towards the [111] direction allows us to obtain an InAs quantum-wire array with width and period of about 300 Å. Therefore, polarization charges are generated at the step edges. We thus have qualitatively realized the theoretical example discussed above and now have experimental access to the phenomenon of lateral piezoelectric fields.

We report on a set of three typical samples with different thicknesses of the InAs layer. The parameters of the (110) and the corresponding (100) reference samples are given in Table II. First, we direct our attention to the HRDXD spectra of the (110) samples together with reference sample No. 3(100) displayed in Fig. 6. For all (100) and (110) samples, we observe well-defined *Pendellösung* fringes indicative of high structural quality. The increase in In content from sample No. 1(110) to No. 3(110) results—as expected—in more pronounced and a larger number of observable fringes. Finally, we even observe a clearer and better defined pattern for sample No. 3(110) than for No. 3(100). This observation clearly underlines the structural perfection of our (110) samples.

In order to find the first fingerprints of the expected strong internal electric fields, we show in Fig. 7 the photoluminescence (PL) spectra of all investigated samples. The spectra of the (100) samples exhibit an extremely strong dependence on the excitation density whereas the (100) spectra remain virtually independent of this parameter. Therefore two spectra at different excitation densities are shown for the (110) and only one spectrum for the (100) samples. Due to the low In content of samples No. 1(100) and No. 1(110), the respective spectra are dominated by the GaAs free-exciton emission at 1.515 eV and a broad band originating in the n^+-doped GaAs substrate, respectively. In addition, we observe in both cases C-related features at about 1.49 eV. For the samples with higher In content the InAs-related emission is the dominating feature. The energy and linewidth of all (100) reference samples compare favorably with studies carried out previously on such structures.[20,21]

In which way do the internal fields manifest themselves in the PL spectra? For all (110) samples, we see a clear blueshift of the PL peak with increasing excitation density. This blueshift ranges from a few meV in sample No. 1(110)—where no definite value can be given due to partially superimposed substrate- and InAs-related peaks—to striking 22 meV for sample No. 2(110). This observation contrasts with a shift of zero in the (100) reference samples and can be understood by the presence of strong internal electric fields in the (110) samples which at larger excitation densities are screened out by photogenerated carriers.[1] Since lateral fields can act across larger distances than vertical fields, they create larger potential

TABLE II. Parameters of the investigated single quantum well (110) and (100) InAs/GaAs samples. High- and low-excitation densities are 30 W/cm^2 and 3 mW/cm^2 for sample Nos. 2 and 3 (Ref. 25).

		E_{PL} (eV)		FWHM (meV)	
Sample No.	d_{InAs} (Å)	Low I_{exc}	High I_{exc}	Low I_{exc}	High I_{exc}
1 (110)	1	1.498			
1 (100)	1	1.504	1.504	3.2	3.2
2 (110)	2	1.457	1.479	25	13.7
2 (100)	2	1.484	1.484	4.1	4.1
3 (110)	3	1.423	1.438	26.3	15
3 (100)	3	1.450	1.450	8	8

differences and thus have a larger impact on the electronic structure. This is underlined by the fact that comparable (311) and (211) InAs/GaAs structures with vertical fields across a few Å instead of lateral fields across hundreds of Å as in the present case exhibit blueshifts which range from unobservable[21] to at most a few meV.[22] Contrary to the case of vertical fields, the observed blueshift does not increase with the quantum-well thickness, which points to the intricate dependence of lateral field effects on the microscopic configuration of the quantum well.

Second, again in strong contrast to the (100) case, we observe a reduction of the PL linewidth with increasing excitation density. An increase of the PL linewidth with increasing electric-field strength is a familiar feature of standard (100) heterostructures under external electric fields.[23] It is therefore reasonable to assign the linewidth reduction observed here also to the screening of the internal piezoelectric fields by photogenerated carriers. With blueshift and linewidth reduction upon increase of the excitation density, we thus observe two features which strongly imply the presence of internal electric fields in our (110) samples.

Since external fields are known to induce an enhancement of the radiative lifetime in (100) heterostructures,[23] it is an interesting test for our hypothesis of lateral piezofields to investigate the temporal emission characteristics of our (110) structures. Figure 8 displays the temporal evolution of the PL peak of sample No. 3(110) after pulsed excitation at 1.530 eV. We see a pronounced spectral diffusion of about 10 meV to the red. Two sources can contribute to this spectral redshift. The first influence certainly is the number of carriers which decreases in the course of time and leads to a less efficient screening of the internal fields. But the inset of Fig. 8 demonstrates a strong dependence of the radiative lifetime on the PL energy which also contributes to the observed spectral diffusion. For the low-energy part of the PL emission, we observe a purely exponential decay—as it is normally seen in (100) InAs/GaAs structures[20]—with a decay time of 750 ps, whereas for the high-energy

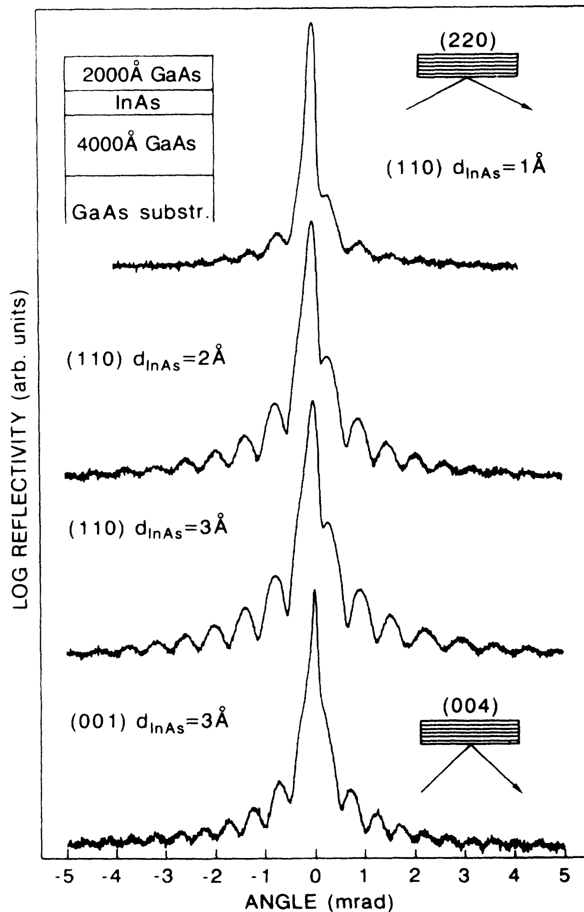

FIG. 6. High-resolution double-crystal x-ray diffraction patterns of all (110) samples and one (100) sample taken in the vicinity of the GaAs (220) and (004) reflections.

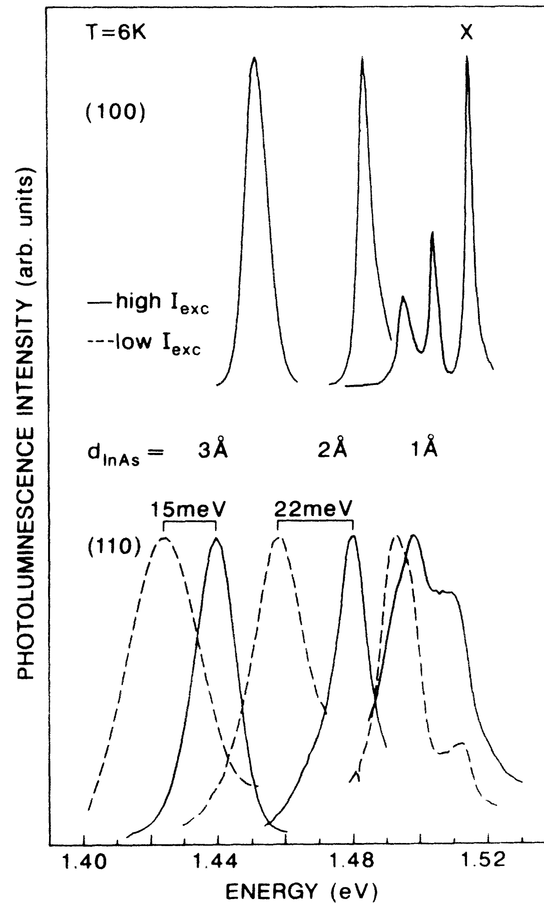

FIG. 7. Photoluminescence (PL) spectra for three (110) and (100) samples with different In content. For the (110) samples, we show spectra taken at an excitation density of 3 mW/cm^2 and 30 W/cm^2 (Ref. 25).

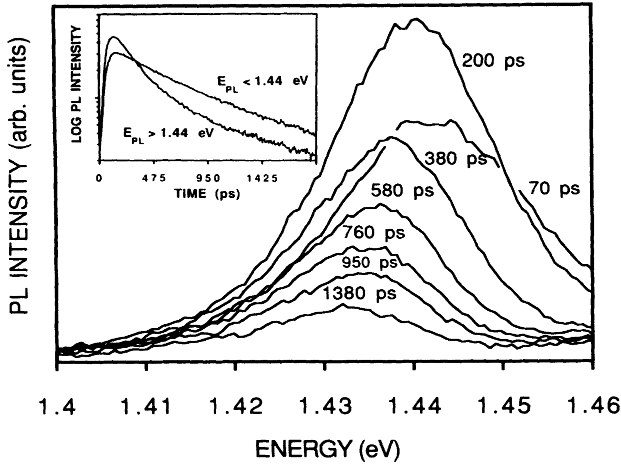

FIG. 8. Transient PL spectra of the 3-Å (110) sample after pulsed excitation at 1.55 eV. The spectra are taken at different delay times after arrival of the pulse, as indicated in the figure. The inset shows the time dependence of the emission spectrally integrated over the low-energy ($E_{PL} < 1.44$ eV) and the high-energy part of the PL line ($E_{PL} > 1.44$ eV) in order to reveal the energy dependence of the radiative lifetime.

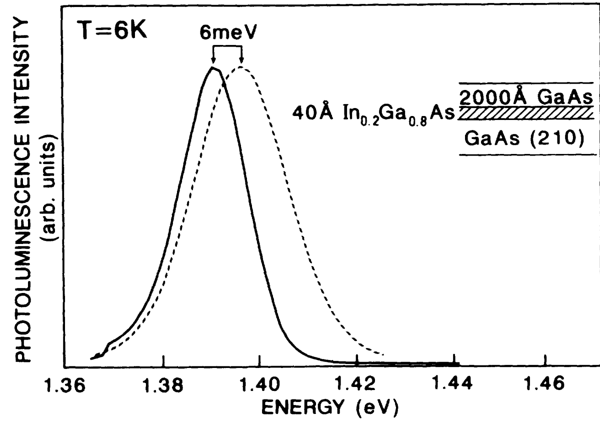

FIG. 9. Photoluminescence spectra of a 40-Å (210) $In_{0.2}Ga_{0.8}As/GaAs$ quantum well. The blueshift of the luminescence is due to lateral piezoelectric fields generated by interface fluctuations.

part a biexponential decay with an initially much shorter decay time of only 250 ps is observed. This difference in decay time can be attributed to the distortion of the wave functions by the internal electric fields. Therefore, the electron-hole overlap for low-energy states is reduced compared to the high-energy states for which the internal fields are screened out. A decrease of the overlap, however, increases the radiative lifetime and results in the observed variation of the lifetime with energy. The time-resolved measurements give additional support to our conclusions above. However, we emphasize that the observation of a prolonged low-energy lifetime is only a necessary, but not a sufficient condition for the existence of lateral fields. Nevertheless, the combination of the two spectroscopic methods is a clear demonstration of the existence and importance of lateral piezoelectric fields.

C. Strained structures with other non-(100) orientations

After the controlled introduction of lateral piezofields in the last section, we now present examples where lateral piezofields are the result of interface fluctuations. We first turn to the PL spectra of a (210) $In_xGa_{1-x}As/GaAs$ sample shown in Fig. 9. For this growth direction the polarization is oriented parallel to the interfaces along the [001] axis. Therefore, the corrugation present on this surface[18] cannot create piezoeffects, since it is also oriented along the [001] direction. The blueshift of 6 meV observed in Fig. 9 therefore is exclusively caused by interface fluctuations. We emphasize that the (100) reference structures do not exhibit this blueshift.

A second, very illustrative example is given by the (311) InAs/GaAs system. For heterostructures with this orientation the data of Fig. 2(c) predict a large value for the lateral component of the piezoelectric polarization. We have the possibility to interrupt the growth of the InAs film just after the transition of the 3D-growth mode.[24] As illustrated in Fig. 10, the film at this stage has an agglomerated morphology and therefore exhibits a pronounced lateral structure of the interfaces. During

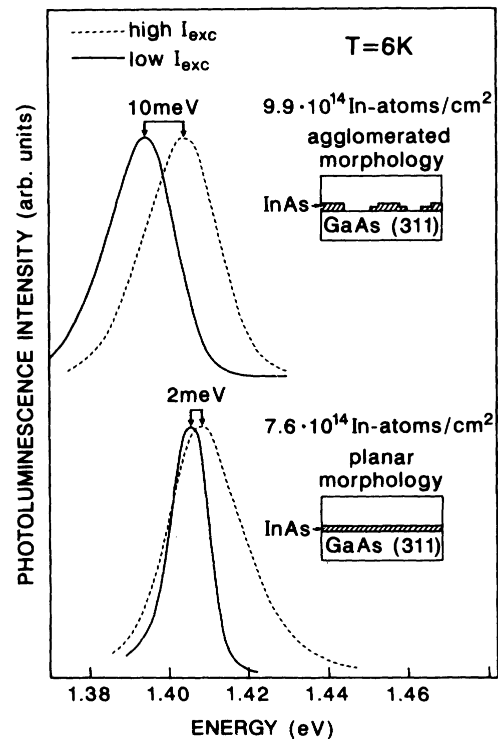

FIG. 10. Photoluminescence spectra of two (311) InAs/GaAs heterostructures. Sample *A* contains a planar InAs film, whereas in sample *B* a film with agglomerated morphology was inserted by growth slightly beyond the critical thickness.

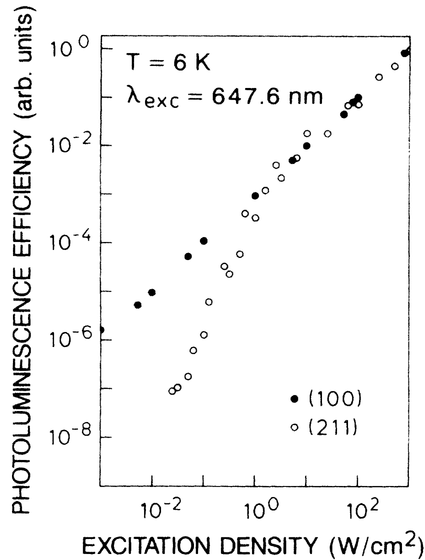

FIG. 11. Dependence of the luminescence intensity of a ten-period 1.2-ML (211) InAs/GaAs-superlattice structure on the excitation density. For comparison the behavior of a (100) reference structure in the same range is also shown.

the overgrowth of the InAs layer with the GaAs cap, we observe a quick recovery of the RHEED pattern. We, therefore, end up with an InAs quantum well, which shows an inhomogeneous distribution of In but nevertheless has an acceptable optical quality.

In Fig. 10, we compare sample A grown in this way with a reference sample B of planar morphology. Sample B was prepared under identical conditions but the InAs growth was interrupted just before the 2D-3D transition started in order to preserve the planar morphology. As expected the PL line of sample B shows only an insignificant dependence on the excitation density. The observed shift of 2 meV approximately corresponds to the value expected theoretically in the presence of vertical fields only. The behavior of sample A is very different, however. Although the In content was increased only slightly in comparison to sample A, the blueshift increases dramatically to 10 meV. This value cannot be explained by the presence of vertical fields only. It is, therefore, caused by lateral piezoelectric fields introduced by a pronounced lateral structure of this InAs film. Again, we do not see this effect when carrying out an equivalent experiment with (100) structures.

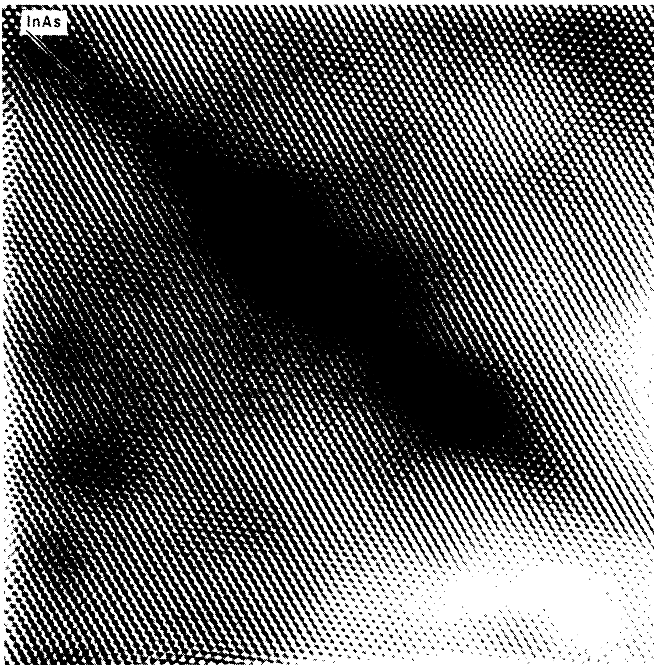

FIG. 12. Cross-sectional HREM picture (300×300 Å) of a 1-ML (211) InAs film taken in the $[01\bar{1}]$ direction.

As a final example, we turn to a 1.2 ML (211) InAs/GaAs sample. With this structure, we show that lateral piezoelectric fields caused by interface fluctuations can lead to a nonlinear dependence of the PL intensity on the optical excitation density. The luminescence line of this sample shifts by about 3 meV when the excitation density is varied between 0.1 W/cm^2 and 1 kW/cm^2.[26] This value of the blueshift can be explained by the presence of vertical piezoelectric fields in conjunction with the occurrence of In segregation during growth.[9] Besides the blueshift, however, this sample also shows a strongly nonlinear dependence of the luminescence intensity on the excitation density.

Figure 11 shows the luminescence intensity to be proportional to $I^{2.6}$ for small excitation densities while at higher densities we have a transition to the standard linear behavior. Calculations show that vertical fields have only insignificant influence on the optical matrix elements in this ultrathin structure. The observed behavior, therefore, cannot be explained by the presence of vertical fields only. We also can exclude the influence of nonradiative centers because the quality of the GaAs barriers was optimized according to the procedure given in Ref. 21. In addition, these nonlinearities cannot be observed in all (211) samples. Therefore, a link has to exist with the interface structure of the sample. Figure 12 shows a cross-sectional high resolution electron micrograph of this sample taken in the $[01\bar{1}]$ direction. This micrograph shows that this film was fragmented during the growth process by slightly too high temperatures during the flash-off step.[20,26] The resulting clusterlike film morphology now acts as a source of lateral piezoelectric fields and provides the explanation for the observed nonlinear behavior.

IV. CONCLUSIONS

We have theoretically introduced and experimentally demonstrated the concept of lateral piezoelectric fields. In the theoretical section, we pointed out that lateral fields can be found in almost all strained III-V and II-VI heterostructures. We emphasized their huge potential for optical nonlinearities due to their easy screenability and the decoupling of the field structure from the critical

thickness of the strained layers. In the experimental part, we first investigated a (110) InAs quantum-wire structure. After a confirmation of the structural perfection of our samples optical experiments produced strong evidence for lateral piezoelectric fields. Evidence for lateral fields was then also revealed in strained structures with orientations different from [110]. The entirety of our experimental results not only unambiguously proves the existence of lateral piezoelectric fields, it furthermore shows their importance for the understanding of strained III-V and II-V heterostructures. In addition, it represents an extremely attractive concept for artificial materials with custom-designed optical nonlinearities.

ACKNOWLEDGMENTS

We would like to acknowledge the expert help of A. Fischer with molecular-beam epitaxy growth and to thank A. Heberle for the time-resolved measurement. Part of this work was sponsored by the Bundesministerium für Forschung und Technologie of the Federal Republic of Germany.

---

[1]C. Mailhiot and D. L. Smith, Phys. Rev. B **35**, 1242 (1987).
[2]D. L. Smith and C. Mailhiot, J. Appl. Phys. **63**, 2717 (1988).
[3]B. Laurich, K. Elcess, C. Fonstad, J. Beery, C. Mailhiot, and D. Smith, Phys. Rev. Lett. **62**, 649 (1989).
[4]E. Caridi, T. Chang, K. Goossen, and L. Eastman, Appl. Phys. Lett. **56**, 659 (1990).
[5]R. Andre, C. Deshayes, J. Cibert, L. S. Dang, S. Tatarenko, and K. Saminadayar, Phys. Rev. B **42**, 11 392 (1990).
[6]L. Xu, X. Chang, D. Auston, and W. Wang, Appl. Phys. Lett. **59**, 3562 (1991).
[7]M. P. Halsall, J. E. Nichols, J. J. Davies, B. Cockayne, and P. J. Wright, J. Appl. Phys. **71**, 907 (1992).
[8]H. Shen, M. Dutta, W. Chang, R. Moekirk, D. Kim, K. Chung, P. Ruden, M. Nathan, and M. Stroscio, Appl. Phys. Lett. **60**, 2400 (1992).
[9]P. Castrillo, M. I. Alonso, G. Amelles, M. Ilg, and K. Ploog, Phys. Rev. B **47**, 12 945 (1993).
[10]M. Ilg and K. H. Ploog, Appl. Phys. Lett. **62**, 997 (1993).
[11]W. G. Cady, *Piezoelectricity* (McGraw-Hill, New York, 1946).
[12]This set of orientations contains the singular [100], [111], and [110] directions and ensures the presence of the technologically important (110) cleavage planes.
[13]L. de Caro and L. Tapfer, Phys. Rev. B **48**, 2298 (1993).
[14]J. Jackson, *Classical Electrodynamics* (Wiley, New York, 1975).
[15]These "lines" can meander in a quite irregular way, depending on the lateral interface structure.
[16]S. Hasegawa, M. Sato, K. Maehashi, H. Asahi, and H. Nakashima, J. Cryst. Growth **111**, 371 (1991).
[17]R. Nötzel, L. Däweritz, N. N. Ledentsov, and K. Ploog, Appl. Phys. Lett. **60**, 1615 (1992).
[18]R. Nötzel, D. Eissler, and K. Ploog, J. Cryst. Growth **127**, 1068 (1993).
[19]M. Krishnamurthy, M. Wassermeier, D. R. M. Williams, and P. M. Petroff, Appl. Phys. Lett. **62**, 1922 (1993).
[20]O. Brandt, L. Tapfer, K. Ploog, R. Bierwolf, M. Hohenstein, F. Philipp, H. Lage, and A. Heberle, Phys. Rev. B **44**, 8043 (1991).
[21]M. Ilg, M. I. Alonso, A. Lehmann, K. H. Ploog, and M. Hohenstein, J. Appl. Phys. **74**, 7188 (1993).
[22]M. Ilg, O. Brandt, and K. Ploog, Appl. Phys. Lett. **61**, 441 (1992).
[23]H.-J. Polland, L. Schultheis, J. Kuhl, E. O. Göbel, and C. W. Tu, Phys. Rev. Lett. **55**, 2610 (1985).
[24]F. Houzay, C. Guille, J. M. Moison, P. Henoc, and F. Barthe, J. Cryst. Growth **81**, 67 (1987).
[25]For sample No. 1, we used 3 W/cm^2 and 30 mW/cm^2 because the low In content of these samples does not allow the observation of a well-defined, InAs-related PL peak outside of this range.
[26]M. Ilg, O. Brandt, A. Ruiz, and K. Ploog, Phys. Rev. B **45**, 8825 (1992).

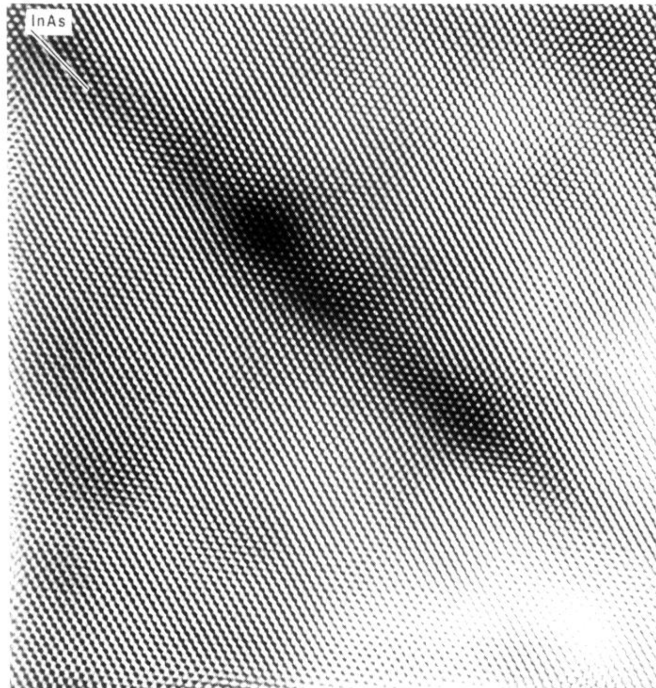

FIG. 12. Cross-sectional HREM picture (300×300 Å) of a 1-ML (211) InAs film taken in the $[01\bar{1}]$ direction.

without piezoelectric field:

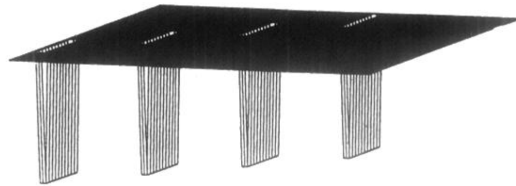

with piezoelectric field:

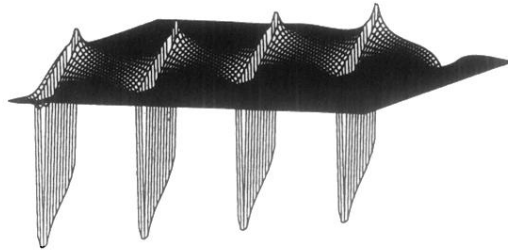

FIG. 4. Potential surface of a $[01\bar{1}]$ cross section through a (110) $In_{0.5}Ga_{0.5}As$ quantum-wire structure with and without lateral piezoelectric fields. The wire width is 200 Å and the thickness 4 Å. The potential term Φ_{piezo} was multiplied by a factor of 5 for illustrative purposes.

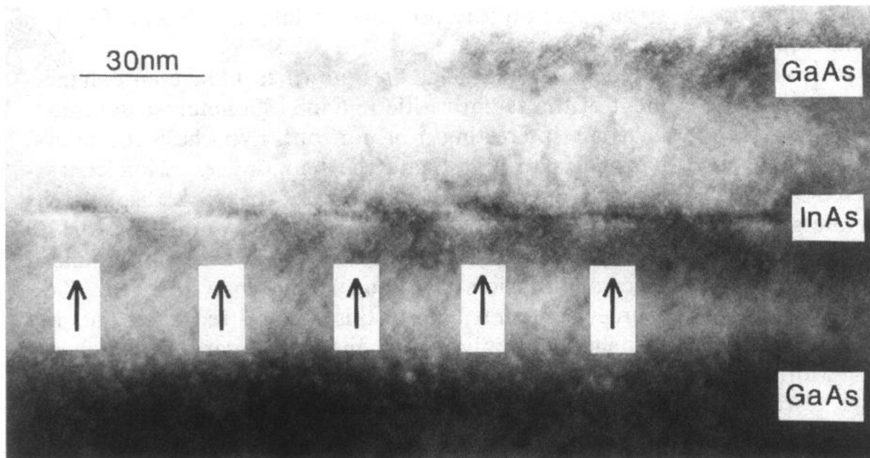

FIG. 5. TEM micrograph of the 3-Å (110) sample realizing the quantum-wire structure. The lateral periodicity of 300 Å of the InAs quantum wires can be seen clearly.